Disk Generator Working With Cesium Seeded Helium

Author(s): P. Karavassilev, L. H. Th. Rietjens, and A. Veefkind

Session Name: Closed Cycle Disk Generators, Part B

SEAM: 26 (1988)

SEAM EDX URL: https://edx.netl.doe.gov/dataset/seam-26

EDX Paper ID: 1286

DISK GENERATOR WORKING WITH CESIUM SEEDED HELIUM

P. Karavassilev, L.H.Th. Rietjens and A.Veefkind
Eindhoven University of Technology, Eindhoven, The Netherlands

ABSTRACT

An experimental investigation of a 4.85 l radial disk generator has been carried out with the Eindhoven shock tunnel facility using cesium seeded helium as working medium. A considerable electrical power density (54.8 MWe/m^3) was obtained at low stagnation pressure (2.9 bar) and low stagnation temperature (1900 K). In all experiments plasma nonuniformities were observed. The enthalpy extraction was limited to 6.1 % due to gasdynamical shocks appearing particularly at the channel inlet and the channel exit. The helium flow turned out to be very sensitive to the magnetic interaction. A quasi-onedimensional gasdynamical analysis was employed using the measured radial current and the measured Hall field radial profile as input, to describe the conversion proces in the disk generator.

INTRODUCTION

The experimental investigations of shock tube driven noble gas disk generators have shown the possibility of high enthalpy extraction. For argon seeded with cesium the advantage of the disk generator with swirl vanes compared to the radial disk generator[1,2] has been confirmed and a high enthalpy extraction (17 %) has been achieved at a relatively low stagnation pressure (4.2 bar) and temperature (2100 K) in spite of the observed nonuniformities in the plasma[3].

The electricity generation at conditions of fully ionized seed was first demonstrated using a radial disk generator with potasium seeded argon[4]. Great performance capabilities of radial disks were reported during the the last years for potasium seeded helium: enthalpy extractions of 12-20 % at stagnation temperatures of 2000-2400 K and stagnation pressures of 2.1-2.6 bar. These results were obtained in the regime of fully ionized seed[5,6]. There are, however, indications that such a regime is limited and that

relatively small variations in the operating conditions may lead to plasma instabilities[7,8].

The aim of the present study is to analyze the performance of a radial disk generator with cesium seeded helium as working medium under different operating conditions yielding nonuniform plasmas.

EXPERIMENTAL SET-UP

The experiments were performed using the shock tunnel facility at the Eindhoven University of Technology[9]. The desired operating conditions for the generator were produced and controlled in a similar way as described in [3]. Details of the shock tube operation when helium is employed as a test gas will be disscussed later.

A section of the generator together with the positions of the diagnostics and the loading circuit is shown schematically in fig.1,a. The radial variation of the cross section is shown in fig.1,b. Single loading was applied in two schemes that are indicated in the figure:

1) between the grounded anode A_1 with radius 45 mm and the cathode C at radius 259 mm;

2) between the floating anode A_2 at radius 91 mm and the cathode C.

In the first case the radial current passes through the nozzle. The volume of the generator, including the supersonic part of the nozzle, is 5.09×10^{-3} m^3.

In the second case the inlet region of the generator works at open circuit and the actual generating volume between A_2 and C is 4.85×10^{-3} m^3.

The crossection of the nozzle throat is 4.216×10^{-3} m^2 and its radial position is 61 mm. At the end of the nozzle (radius 85 mm) the Mach number is 2.7.

Downstream of the cathode at a radius of 287 mm the flow enters a diffuser region equiped with diffuser wedges[3].

A number of diagnostics was applied to the generator for the determination of the flow characteristics and plasma parameters. The static pressure was monitored by means of piezo-resistive pressure transducers on five radial positions dispersing slightly from each other in azimuthal direction. Stainless steel rings similar to those of the anode A_2 and the cathode served as voltage probes[3]. During operation according to the first scheme of loading the ring A_2 was also used as a voltage probe (V_0 in fig.1,a).

Two optical ports, on radial positions 131 mm and 151 mm (2.7 rad apart azimuthally), were used for detection of the plasma radiation. Through the inner port the cesium transition $6d^2D_{3/2}$-$6p^2P_{1/2}$ with wavelength 876,1 nm was monitored and through the outer port both the cesium transition $9d^2D_{3/2}$-$6p^2P_{1/2}$ with wavelength 566,4 nm and the recombination continuum radiation with wavelength 490.0 nm, emmitted from one single spatial area. The measurement of both spectral line intensities was used to determine the plasma fluctuation level, while the ratio of the light intensities, detected through the outer optical port was employed for the electron temperature determination by means of the line to continuum ratio method[11]. The optical signals were sampled with 250 kHz by a multiwaveform digitizer. The other signals were sampled with 10 kHz by data loggers. The data acquisition equipment is positioned in a CAMAC crate which is connected to a PDP-11 computer[9].

For some experiments additional information was provided by fast photography. The observations were restricted to a sector of about one radian between radii 65 mm and 175 mm. Streak pictures were made with a total streak time of about 140 μs.

SHOCK TUBE CONDITIONS

The taylored interface mode[10] can not be employed for the experiments considered in this presentation. For hydrogen/helium as driver gas/test gas the stagnation temperature corresponding with the taylored interface condition is 780 K, which is too low for MHD experiments. For the stagnation temperatures of interest the stagnation conditions after the reflection of the shock appear not to be constant. The stagnation pressure is continiously rising during the passage of the test gas through the channel (fig.2a,b). In the figures the test interval is indicated as it is determined from the current generation period. Assuming adiabatic compression after the shock reflection, a correction has to be made for the increase of the stagnation temperature with respect to the value determined by means of the shock propagation velocity[3].

For security reasons the hydrogen pressure in the driver section prior to the rupture of the diafragms was fixed to 5.25 bar. Reasonable stagnation temperatures are then achievable for pressures of the test gas as low as 10 - 25 Torr. The lower value provides an amount of test gas enough only

for about 2.2 ms flow duration. As a result the test interval at such conditions was restricted to about 0.5 ms (fig.2,a). In the figure 2.b it is seen that a larger amount of test gas increases the flow duration and the lenght of the test interval. It is seen also that for P_{test}=25 Torr the adiabatic compression is almost completed to the beginning of the test interval. The contribution of the compression to the increase of the stagnation temperature is in that case larger than in the case of P_{test}=10 Torr. In general the additional compression of the test gas after the shock reflection leads in practice to a reduced decrease of the stagnation temperature with increasing test gas pressure.

RESULTS AND ANALYSIS

The performance of the radial disk generator was investigated at quasi-stationary operating conditions for a test interval of at least ten flow times. The magnetic induction, the seed fraction and the load were varied independently. This was not possible for the stagnation pressure and the stagnation temperature because of the fixed pressure of the driver gas. The operating conditions are listed in Table 1.

Table 1. Operating conditions

	anode upstream of the nozzle	anode downstream of the nozzle
magnetic induction	0.85 - 3.35 T	1.1 - 2.8 T
seed fraction	0.005 - 0.25 %	0.01 - 0.11 %
load resistance	0.032 - 2.40 Ohm	0.033 - 7.18 Ohm
stagnation temperature	2600 K	1850 - 2100 K
stagnation pressure	2.1 bar	3.5 - 2.6 bar

Shock formation

The radial distribution of the static pressure, as observed in the generator without magnetic interaction at different stagnation conditions, suggested the presence of gasdynamical shocks. We have employed a simplified flow representation assuming oblique shocks on three radial positions. Shock relations similar to those in a linear flow have been applied to calculate the gasdynamical discontinuities.The corners on the generator walls at radial positions 85 mm and 250 mm (fig.1,b) are likely to cause gasdynamical shocks at these positions. Moreover, the fast increase of the channel crossection as displayed also in figugure 1,b, may cause a development of an oblique shock in the middle part of the channel. For the reasones mentioned above the shock locations are chosen at R = 85, 190 and 250 mm.The quasi-onedimensional calculations without magnetic interaction including gasdynamical shocks at the mentioned positions in the channel, with shock angles of 0.6 radian for the first and 0.46 ragian for the downstream shocks, yield static pressure radial profiles fitting the measured ones. An example is presented in figure 3. The horizontal bars in the figure account for the diameters of the orifices leading to the pressure transducers. The vertical bars result from three different sorces of error. These are the Mach number variation over the orifice, the inaccuracy of the detection equipment and the pressure fluctuations. The first source dominates in the supersonic nozzle region and gives a large static pressure uncertainity at the monitored radial interval, corresponding to the large Mach number variation. Along the channel the contribution of the Mach number uncertainity to the static pressure error decreases quickly, the other two sorces being almost constant. The pressure fluctuations appear to be the dominating sorce of error in the downstream half of the channel.

Under conditions of power generation the helium flow experiences both the gasdynamical shocks and the flow deceleration due to the magnetic interaction. The shocks are assumed to keep the same radial positions as for the case of low magnetic interaction, but their angles are assumed to change according to the strength of the maghetic interaction, the limit being normal shocks.For example, in an experiment with electrical power of 124 kWe carried out at approximately the same stagnation conditions as those indicated in figure 3, the calculated pressure profile fitting the experimental static pressure corresponds to shock angles of about 0.65 radian in the downstream half of the channel. In our experiments the limit of normal shock formation was not achieved even at the strongest flow

decelerations which could be obtained with the available values of the operating parameters (magnetic field, seed fraction, load resistance).
An example of a gasdynamical shock in the generator flow with magnetic interaction is shown in figure 4, which presents a streak photograph of the generator for an experiment with power output of 180 kWe. In this figure the kinks in the streamer tracks at radial position of about 120 mm indicate a sudden decrease of the flow velocity due to an oblique shock at that position.

Electrical performance

The dependence of the output power on the magnetic induction for two values of the seed fraction is presented in figure 5. In the figure the curves 1 and 2 are obtained with the load connection between A_2 and C and curves 3 and 4 with the load connection between A_1 and C (see fig.1,a for the positions of the electrodes). The decrease of the electric power which eventually occurs when magnetic induction increases is attributed to the flow deceleration due to the magnetic interaction. This conclusion is supported by the observed simultaneous increase of the static pressure and decrease of the Hall field, particularly in the downstream half of the channel. For the conditions considered in figure 5 we may state that for seed fractions as low as 0.02% no gain in the output power can be obtained by increasing the magnetic induction above 2.0 T. For higher seed fractions the power becomes smaller, as we can see from figure 5 comparing the curve 1 with curve 2 and curwe 3 with curve 4. Also this effect has been attributed to the flow deceleration. Voltage to current characteristics of the generator are presented in figure 6. In this figure the points of the curves 1 and 2 are obtained with the load connection between A_2 and C while the points of the curve 3 are obtained with the load connection between A_1 and C (see fig.1,a). The correcponding operating conditions are indicated in the figure. The shape of the curves is determined from a combination of two effects:
i) the influence of the current on the electrical conductivity and on the Hall parameter;
ii) the influence of the magnetic interaction on the induced voltage.
Presuming that the variations of the effective Hall parameter are not too large, it follows from the generalized Ohms law that the relatively large values of the derivative dI_r/dU_{Hall} of the V-A curve may be caused by

relatively large values of the average effective conductivity or by relatively large values of the radial flow velocity (the latter being the cause for larger open circuit voltages). Curve 2 applies to measurements at a low seed fraction. It may be expected that this curve is mainly determined by the effect of the magnetic interaction on the flow velocity. Because the azimuthal current density (and consequently the Lorentz force) decreases when the radial current density increases, the flow velocity will increase. As a result the value of dI_r/dU_{Hall} is indeed expected to increase with the radial current as we see in the figure. The curves become more complicated when they are partially determined by the effect of the current on the conductivity. Comperatively large values of the conductivity are expected near the open circuit conditions where the total current density becomes maximal.

In none of the conditions applied, the fluctuation measurements have indicated operation of the generator with uniform plasma and fully ionized seed.

At the relatively high stagnation temperature of 2600 K the enthalpy extraction appeared to be limited to a value of 4.7 %. At a stagnation temperature of 1900 K the enthalpy extraction was 6.1 %, the maximum for the experiments considered here. The reason for the lower enthalpy extraction at the higher stagnation temperature was presumably the related lower stagnation pressure, as it was discussed in the section concerning the shock tube conditions. The stagnation pressure appeared to become so low that the flow deceleration has serously reduced the output power.

The azimuthal current value appears to be an important additional check for he calculated values of the effective conductivity and effective Hall parameter by means of the quasi-onedimensional model used, as it is disscused in 3. For some experiments the total azimuthal current was measured by measns of a Rogovsky coil. The calculated values for the total azimuthal current at the conditions of the experiments,concerning the V-A characteristics of the generator, agree with the experimentaly measured values in the limits of the errors assumed.

CONCLUSIONS

Experiments with a radial disk generator employing cesium seeded helium as the working medium have been carried out under different operating

conditions (seed fraction, magnetic induction, load resistance, stagnation temperature, stagnation pressure). During all experiments the plasma was observed to be nonuniform. A maximum electrical power density of 54.8 MWe/m^3 was obtained at a stagnation temperature of 1900 K and a stagnation pressure of 2.9 bar.

For shock tube experiments involving helium as the test gas the desired entrance conditions for MHD generators do not match with the requirements for the tailored interface mode operation of the shock tube. As a result the stagnation pressure as well as the stagnation temperature increase after the shock reflection. This effect had to be taken into account when evaluating the data.

The performance of the generator appeared to be strongly affected by gasdynamical effects. The measured pressure distriburion along the channel indicated the presence of gasdynamical shocks already in the flow without magnetic interaction. These shocks have been attributed to the shape of the duct wall. For a flow with magnetic interaction further deceleration was observed from increasing pressures and decreasing Hall fields in the downstream part of the channel. The deceleration of the flow limited the electrical power obtained at large magnetic inductions, large seed fractions and also large stagnation temperatures.

Two schemes of load connection were compared:
(a) a grounded anode upstream of the nozzle;
(b) a floating anode downstream of the nozzle.
With respect to the generator performance no appreciable difference was found.

The shapes of the current to voltage characteristics are determined by a number of effects. Not only the electrical conductivities and Hall parameters may vary with the load resistance, but also the induced voltage. The latter effect is caused by the deceleration of the flow due to the magnetic interaction (which is different for different load resistances) and was clearly observed during the experiments.

ACKNOWLEDGEMENTS

The persistent and valuable help of the shock tunnel facility technical team: inj. A.A. Bierens, H.F. Koolmees, A.H.F.M. Baede and A.W.M. van Iersel is greatfully acknowledged.

REFERENCES

1. Hruby, V.J., "Experimental investigation of the MHD disk generator with inlet swirl", M.S. Engeneer Thesis, MIT, 1976.
2. Loubsky, W.J. et al., "Detailed studies in a disk generator with inlet swirl driven by argon", Proc. 15th Symp. on Eng. Asp. of MHD, Philadelphia, Penns., 1976.
3. Veefkind, A. et al., "Generator performance experiments with a shock tunnel driven noble gas MHD generator", Proc. 9th Int. Conf. on MHD El. Power Gen., Tsukuba, Japan, 1986.
4. Shioda S., Yamasaki H., "Generation experiments with a disk MHD generator under the conditions of fully ionized seed", Proc. 6th Int. Conf. on MHD El. Power Gen., Washington D.C., 1975.
5. Yamasaky, H. et al., "Closed cycle MHD disk experiments at TIT", Proc. 23th Symp. on Eng. Asp. of MHD, Somerset, Call., 1985.
6. Harada, N. et al., "High enthalpy experiments with a closed sycle disk MHD generator", Proc. 9th Int. Conf. on MHD El. Power Gen., Tsukuba, Japan, 1986.
7. Tanaka, D., Hattori J., "Time dependent properties of nonequilibrium MHD generator with fully ionized seed plasma", Proc. 7th Int. Conf. on MHD El. Power Gen., MIT, 1980.
8. Louis, J., "Effects and nature of non-uniformities in nonequilibrium denerators", Proc. 9th Int. Conf. on MHD El. Power Gen., Tsukuba, Japan, 1986.
9. Veefkind, A. et al., "High power density experiments in a shock tunnel MHD generator", AIAA Journal, 14 , 8, 1976, p. 1118-1122.
10. Oertel, H., "Stossrohre", Springer-Verlag, N.Y., 1966.
11. Wetzer, J.M., "Spatially resolved determination of plasma parameters of a noble gas linear MHD generator", Thesis, Eindhoven University of Technology, 1984.

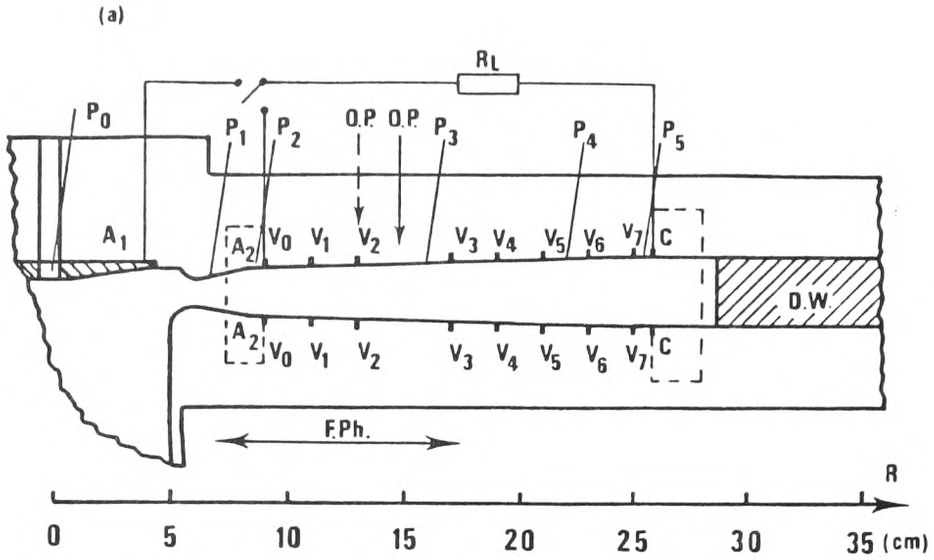

A_1 - anode, oxygen-free copper plate
A_2 - anode
V_0 - V_7 - voltage probes } - stainless steel rings
C - cathode
D.W. - diffuser wedges
R_L - load
P_0 - P_5 - pressure transducers
O.P. - optical ports
F.Ph. - fast phot. rad. range

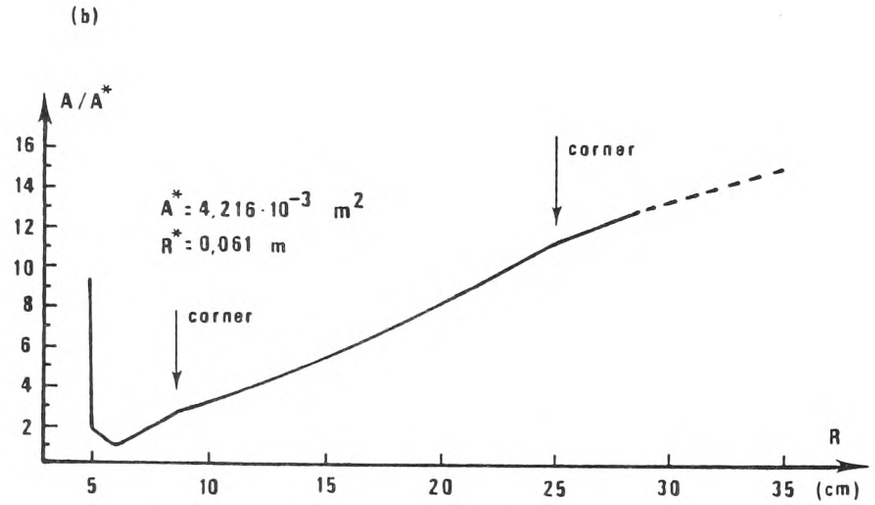

Fig. 1. a) Scheme of a section of the disk generator with the positions of the diagnostics and the loading.
b) Radial variation of the generator cross section A. The throat values are diven as A^* and R^*. The arrows indicate the positions of the wall corners. The dotted line is for the diffuser cross section.

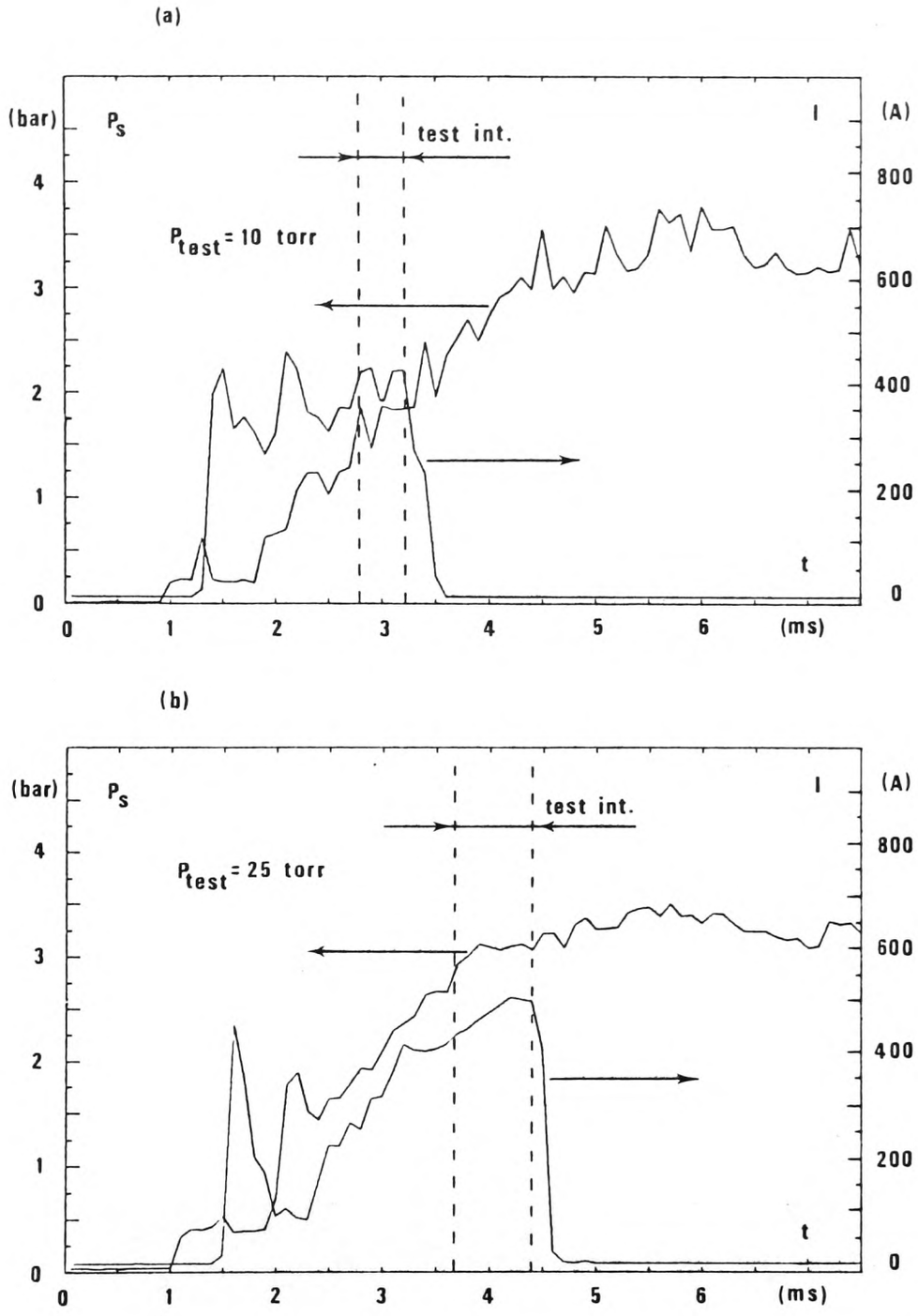

Fig. 2. a) Stagnation pressure (P_s) and Hall current (I) history for a low pressure of the test gas (P_{test}) prior to the rupture of the shock tube diafragmes. The test interval is also indicated.

b) The same quantities at 2.5 times higher pressure of the test gas.

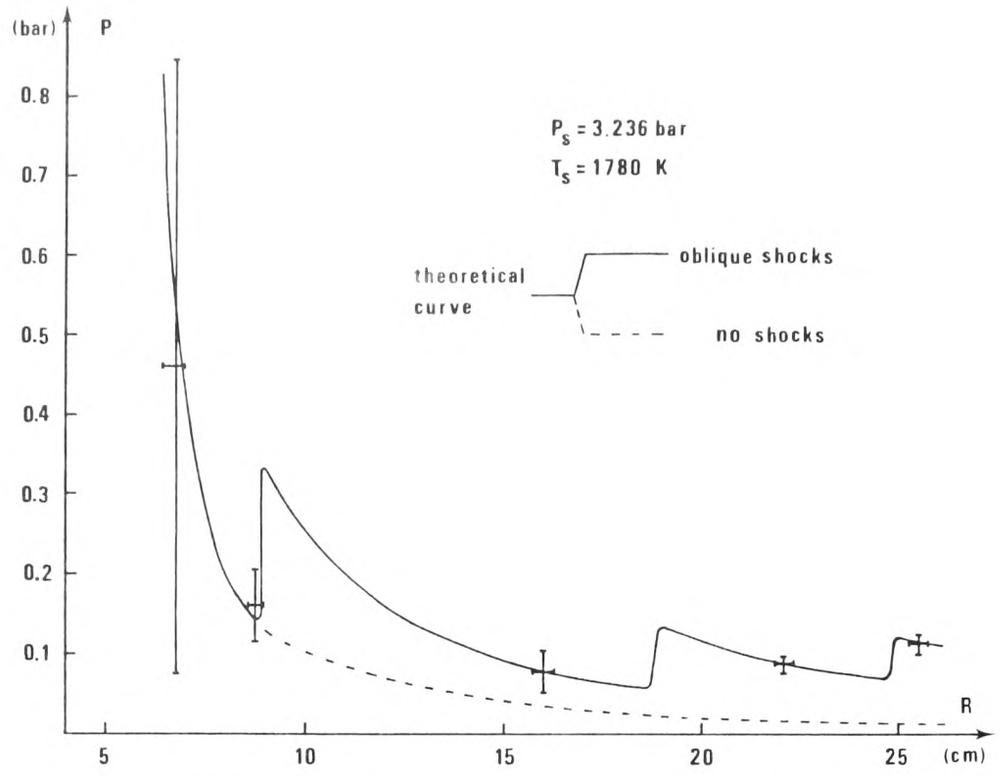

Fig. 3. Calculated radial profile of the static pressure P and experimental values (with their errors) for zero magnetic interaction. The entrance stagnation pressure P_s and stagnation temperature T_s are indicated.

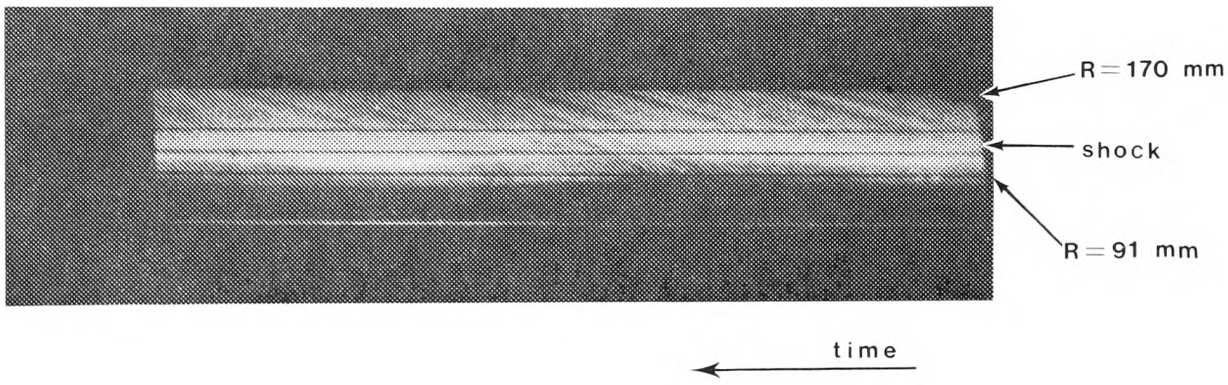

Fig. 4. Streak photograph of the radial disk generator at conditions of considerable magnetic interaction: P_s = 3.05 bar, T_s = 2090 K, B = 1.8 T, R_L = 0.18 Ohm, seed fraction 0.075 %

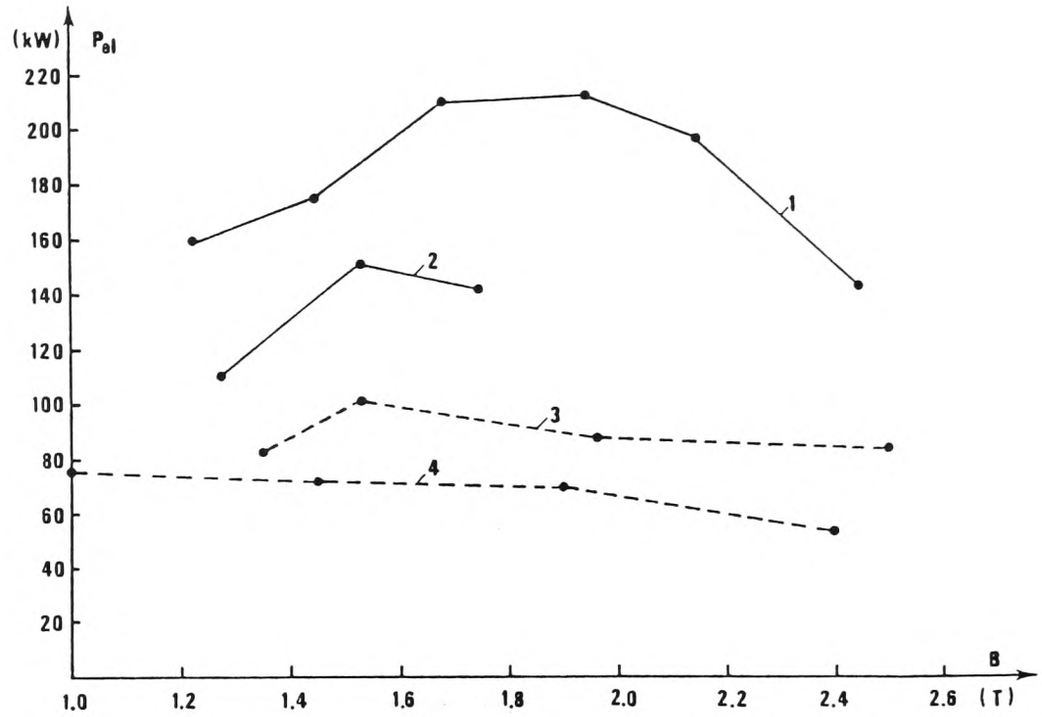

Fig. 5. Output power (P_{el}) versus magnetic induction (B). Curves 1,2: load connected between A_2 and C; curves3,4: load connected between A_1 and C (A_1,A_2,C - see fig.1.a). The operating conditions are:

curve 1 seed fraction 0.02 % } { P_s=2.9 bar, T_s=2130 K,
curve 2 seed fraction 0.045 % } { R_L=0.19 Ohm

curve 3 seed fraction 0.08 % } { P_s=2.15 bar, T_s=2600 K,
curve 4 seed fraction 0.2 % } { R_L=0.50 Ohm

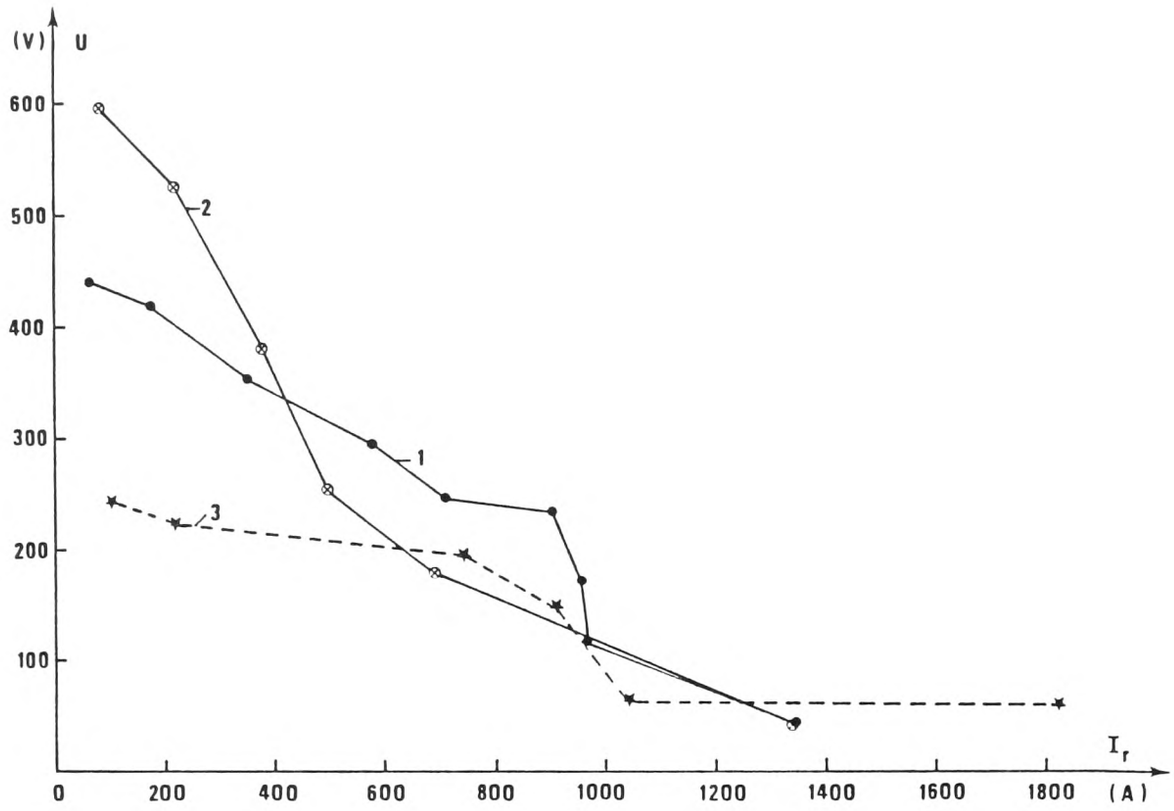

Fig. 6. Voltage to current characteristics of the generator. Curves 1,2: load connected between A_2 and C; curve 3: load connected between A_1 and C (A_1,A_2,C - see fig. 1,a). The operating conditions are:

curve 1 P_s=3.0 bar, T_s=2100 K, B=1.75 T, seed fraction 0.03 %

curve 2 P_s=3.35 bar, T_s=1870 K, B=2.85 T, seed fraction 0.008 %

curve 3 P_s=2.2 bar, T_s=2600 K, B=1.30 T, seed fraction 0.04 %